International Communications in Heat and Mass Transfer 66 (2015) 32–39

Contents lists available at ScienceDirect

International Communications in Heat and Mass Transfer

journal homepage: www.elsevier.com/locate/ichmt

Thermal and optical investigations of high power LEDs with metal embedded printed circuit boards☆

Xinrui Ding, Yong Tang, Zongtao Li *, Qiu Chen, Yuji Li, Yongtai He

Key Laboratory of Surface Functional Structure Manufacturing of Guangdong High Education Institutes, South China University of Technology, Guangdong 510640, PR China

ARTICLE INFO

Available online 16 May 2015

Keywords:
Light emitting diode (LED)
Metal embedded-PCB
Thermal performance
Optical performance

ABSTRACT

To improve the thermal and optical performances for high power LEDs, a metal embedded printed circuit board (MEPCB), with a columnar copper slug inside the low cost FR4 material, was introduced in this paper. This novel structure makes it possible to connect the LED component directly to the outside environment. The thermal performances, including thermal resistances and temperature distributions of the MEPCB were evaluated by employing the finite element analysis method (FEA) and transient thermal measurement. The luminous and chromatic characteristics were also measured and analyzed at transient state and steady state. Results showed that the maximum reductions in the total thermal resistance and junction temperature were 65.60% and 56.25% by using the MEPCB compared with the conventional metal core printed circuit board (MCPCB). Benefiting from the excellent thermal performance of the MEPCB, up to 24.14% increase in steady state luminous flux was obtained compared with the MCPCB. Moreover, the correlated color temperature (CCT) shift value between 150 mA and 900 mA could be controlled within 93 K. This work demonstrates that the MEPCB is more suitable for LEDs working at wide current ranges.

1. Introduction

Light emitting diode (LED) has many advantages including energy saving, long lifetime, sharp response, small size and convenient control [1]. In recent few years, LED was accelerating the revolution in lighting industry from displaying, sensing, to general lighting [2]. However, there are some unavoidable challenges for commercial applications, such as thermal effect. Although LED has a higher transfer efficiency, a fair amount of input power will convert into heat and elevate the junction temperature rapidly, which causes a series of problems of the LEDs [3,4]. Therefore, it is important to dissipate the heat from LED chips as efficiently as possible.

Ceramic, metal, and FR4 are three kinds of popular materials used as printed circuit boards for high power LED assembly. Ceramic is a proper material with good thermal and insulating properties [5–7]. Unfortunately, the fabrication process of ceramic substrate (CS) is complex and cost-consuming. The CS is better fit for high-end applications [8]. Metal core printed circuit board (MCPCB) and insulating metal substrate (IMS) [9,10] usually use high thermal conductivity material, such as aluminum or copper, as heat spreaders to enhance the thermal performance of the PCB board. In order to separate the electrical circuit layer and the metal layer, an inserted insulating layer is necessary. However, the insulating layer is made of epoxy or polyimide with quite low thermal conductivity. It obstructs the heat dissipating route from the circuit layer to the heat spreader layer. Consequently, though the metal layers have good thermal conductivity, the overall thermal performance of the MCPCB is still insufficient. Many researches have been focused on the improvement of this issue. Kim et al. [11] designed a flexible package substrate with thermal via-hole fully filled with copper using a laser drill and electrolytic pulse plating method. Wu et al. [12] developed and analyzed a novel type of MCPCB with blind/through hole by filling with Cu using electroplating. Lee et al. [13] developed patterned anodizing MCPCB which made it possible to connect the LED component to the MCPCB without thermal loss through the insulating layer. Literature [14] reported a SuperMCPCB substrate which combined a direct plating ceramic layer (DPC) and the MCPCB together. The results showed that by replacing the conventional aluminum MCPCB with the SuperMCPCB, the thermal resistance decreased by 1.27 K/W. However, these methods are complex, high cost and lack of marked competitiveness. FR4 is another acceptable material for high power LEDs due to its outstanding cost advantages [15]. The FR4 PCB has high mechanical strength, good electrical insulating qualities in both dry and humid conditions and mature technology, but the thermal conductivity is only 0.3–0.4 W/m-K [16,17], which makes the FR4 layer be the greatest bottleneck in the thermal path of the LED lighting. Therefore, the circuit board is one of the most important issues in the LED thermal management to the best of our knowledge.

An ideal circuit board for high power LEDs should be low-cost as FR4s and high heat-conducting as metals. This is a common object of the lighting manufactories, and lacks of report. In this work, a copper

☆ Communicated by W. J. Minkowycz.

* Corresponding author.
E-mail address: meztli@scut.edu.cn (Z. Li).

http://dx.doi.org/10.1016/j.icheatmasstransfer.2015.05.005
0735-1933/

Nomenclatures

M	Molecular weight of air [g/mol]
P_{atm}	Atmosphere pressure [Pa]
R_{gas}	Universal gas constant [J/(K · mol)]
q	Heat flux [W/m^2]
C_{th}	Thermal capacitance [J]
R_{th}	Thermal resistance [K/W]
c	Volumetric heat capacitance
A	Surface/cross section area [m^2]
P	Power [W]
Φ_v	Luminous flux [lm]
T	Temperature [°C]
u	Uncertainty

Greek symbols

η	Luminous efficiency [%]
ρ	Density of the air flow [kg/m^3]
λ	Thermal conductivity [W/(m · K)]
n	Normal vector along heat flow path

Subscripts

j	Junction
a	Ambient
h	Heat
el	Electrical
opt	Optical
btm	Bottom
ref	Reference

base metal embedded printed circuit board (MEPCB) was developed, which combined the advantages of the PCB and MCPCB. At first, the finite element analysis method was applied to study the temperature distributions. Then, the thermal resistances were investigated using forward voltage method coupled to the transient thermal tester analysis (T3ster®). At last, the electrical, luminous and chromatic performances at different input current had been measured experimentally.

2. Experimental descriptions

2.1. Description of the testing samples

The MEPCB was manufactured by the following processing steps as shown in Fig. 1(a). (1) The FR4 board and the two copper layers were laminated together by heat rolling process. The bottom copper spreader layer was about 200 μm thick and the upside copper circuit layer was about 75 μm thick. (2) The drilling process was carried out to form a hole in the center of the board. (3) A columnar copper slug was embedded in the center hole by a pressing machine. (4) The circuit layer patterning processes were proceeded which consisted of photo resist process, exposure process, etching process and plating process. Here, it is necessary to point out that there is a copper plating layer on the bottom of the MEPCB. This layer filled the gap between the copper slug and the copper spreader layer, which could reduce the contact thermal resistance, enhance the combination strength and improve the sealing performance of the MEPCB. A commercial MCPCB was used as a comparison in this work. In Fig. 1(b), the cross section schematic diagrams illustrate the thickness of each layer of the MEPCB and MCPCB. There was an insulating layer between the circuit layer and aluminum layer in the MCPCB. Differently, there was no heat insulating material blocking in the heat flow path in the MEPCB. The high power LED applied in this work uses GaN-based blue light chip with yellow phosphor (YAG:Ce^{3+}) to produce white light. At the typical power of 1 W with input current of 350 mA, the LED generates neutral white light by mixing the blue light from the LED chip and the yellow light from

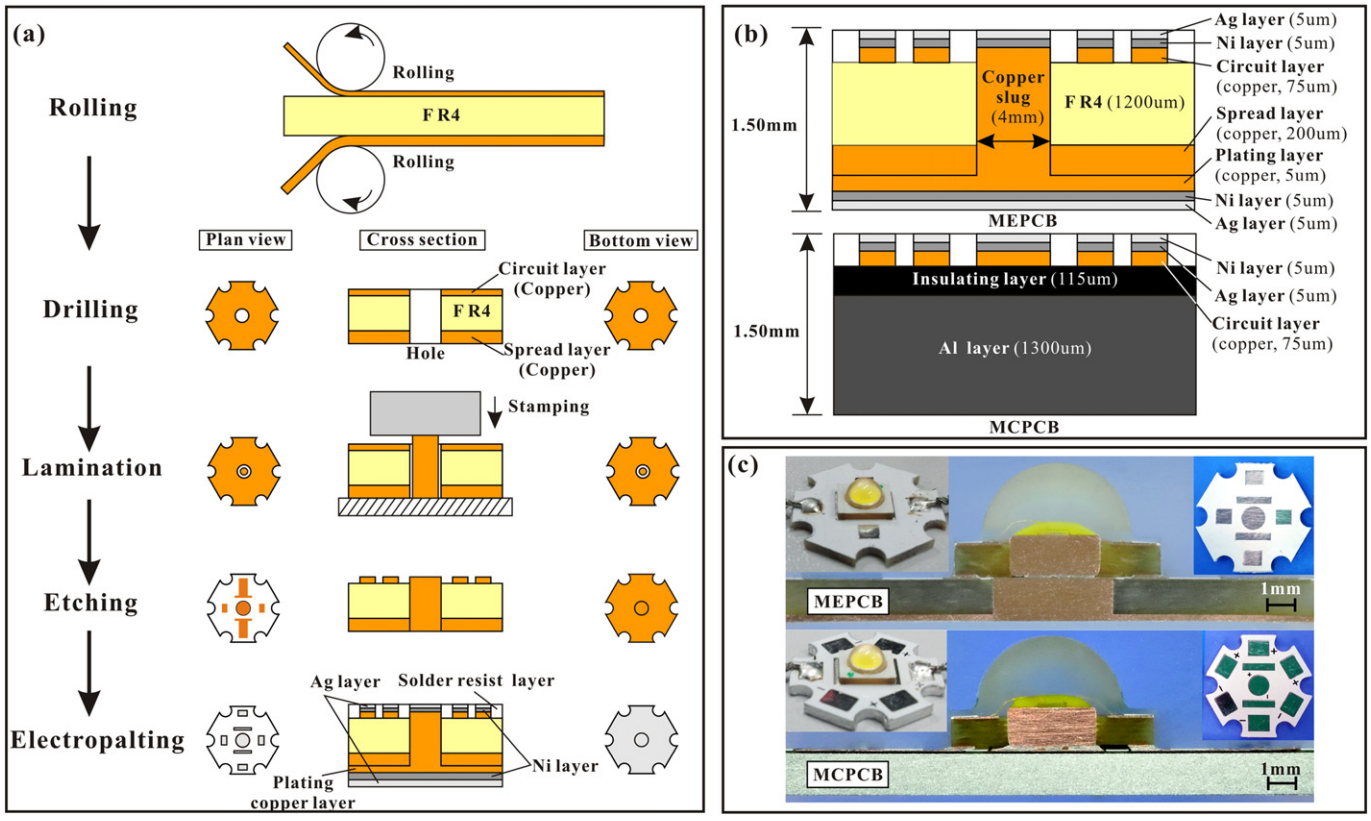

Fig. 1. Schematic diagrams of the MEPCB and MCPCB. (a) Manufactory processes of the MEPCB. (b) Cross section schematic diagrams of the MEPCB and MCPCB. (c) Photos of the MEPCB and MCPCB.

the phosphor. The size of the LED is 6.0 mm width and 7.0 mm length. Finally, the high power LED components were bonded onto the MEPCB and MCPCB with solder SAC 305 by surface mount technology (SMT). The cross section photos of the MEPCB and MCPCB with LED components are shown in Fig. 1(c). The copper slug was well combined with the FR4 and the bottom copper layer.

2.2. FEA simulations

ANSYS® Fluent was used to simulate the thermal performances of the MEPCB and MCPCB. The ambient temperature was set as 25 °C, and the air flow was three dimensional, laminar and steady. The LED components operated under natural convection with a heat consumption of 1 W. The density of the air flow was calculated based on the ideal gas law as below.

$$\rho = \frac{MP_{\text{atm}}}{R_{\text{gas}}T} \tag{1}$$

where M is the molecular weight of air (28.966 g/mol) and R_{gas} is the universal gas constant. The governing conditions during the simulation were set based on mass, momentum and energy conservation equations, which had been introduced in our previous work [18]. A first order upwind scheme was used for the discretization of the inertial terms in the governing equations, offering stable, convergent, and accurate simulations. The boundary conditions were set as follows:

(1) The simulation domain was a 30 × 30 × 20 mm cabinet whose surface type was opening along the gravity direction.
(2) A 1 × 1 mm source was placed on top of the chip with constant heat flux of 1×10^6 W/m^2.
(3) The properties at the air–solid interfaces were as follows:

$$T_{\text{air}} = T_{\text{solid}} \tag{2}$$

$$\mathbf{q} = -\lambda_{\text{air}}\left.\frac{\partial T}{\partial \mathbf{n}}\right|_{\text{interface}} = -\lambda_{\text{solid}}\left.\frac{\partial T}{\partial \mathbf{n}}\right|_{\text{interface}} \tag{3}$$

(4) The thermal conductivities of the materials used in the simulations are listed in Table 1.

2.3. Transient thermal measurements

The schematic of the transient thermal measurement setup is shown in Fig. 2, including a cold plate with temperature controller, a transient thermal tester (T3ster®), a 0.5 m diameter integrating sphere, a spectrometer (Instrument system®) and a computer.

Transient thermal measurement is a non-destructive method to measure the thermal properties of LED component. The relationship between the temperature rise of the junction and the forward voltage, which is known as K factor, can be denoted by Eq. (4).

$$K = \frac{dT_{\text{j}}}{dV_{\text{F}}} \tag{4}$$

$$T_{\text{j}} = K \times \Delta V_{\text{F}} + T_{\text{ref}} \tag{5}$$

where V_{F} is the forward voltage; T_{j} is the junction temperature of the LED chip; and T_{ref} is the temperature of the reference point, which is the cold plate temperature in this work. By extracting the thermal structure function in Eq. (6), the thermal resistance (R_ε) and thermal capacitance (C_ε) of each layer could be identified using the Network Identification De-convolution (NID) method [19–21].

$$\frac{dC}{dR} = c\lambda A^2 \tag{6}$$

where c is the volumetric thermal capacitance, λ is the thermal conductivity and A is the cross sectional area of the flow path. When the temperature became steady during the transient thermal measurement, a 5 mA measurement current was applied to the LED immediately and the forward voltages were recorded. Then, the junction temperature of the LED chip can be calculated by K factor. Each sample was assembled on the cold plate under different thermal interface conditions: air interface condition, or thermal grease interface condition. The detailed measurement was described in JEDEC standard 51–14 [22]. The total uncertainty (u) includes the experimental uncertainty (u_{E}) and numerical uncertainty (u_{N}), and it can be calculated by Eq. (7):

$$u = \sqrt{u_N{}^2 + u_E{}^2}. \tag{7}$$

The total uncertainty of the thermal resistance, junction temperature, luminous flux and color coordinate are 4.73%, 2.15%, 4.03% and 0.0015.

Table 1
Thermal conductivities of materials in FEAs.

Materials	Sapphire	Copper	Aluminum	SAC solder	Insulting layer	FR4
Thermal conductivity ($W \cdot m^{-1} \cdot K^{-1}$)	42	387	217	60	0.5	0.3

3. Results and discussions

3.1. Simulated thermal performances

The simulation results are shown in Figs. 3 and 4. From the cross section view of the MCPCB in Fig. 3(a), it is noted that most of the heat concentrates on the LED component. And there is a distinct temperature boundary between the LED component and the MCPCB, where the low thermal conductivity insulating layer is located. The maximum temperature appears at the LED chip, and it can be regarded as the junction temperature (T_{j}) of the LED chip. For the MCPCB, the T_{j} reaches 101.8 °C. For the MEPCB as shown in Fig. 3(b), the T_{j} of the LED chip is 86.4 °C, 15.4 °C lower than that of the MCPCB. The axonometric views of the MEPCB and MCPCB are shown in Fig. 3(c) and (d). It can be seen that the temperature distribution on the upside surface of the MCPCB is more uniform than that of the MEPCB. However, the main heat dissipation path is not the upside surface but the bottom side of the circuit board [10]. Fig. 4 shows that the highest temperature on the bottom surface is located at the center, and temperatures decrease along radial direction for both samples. The average bottom temperatures ($T_{\text{btm,avg}}$) of the MCPCB and MEPCB are 74.6 °C and 76.4 °C, and the maximum temperature differences on the bottom surface of the MEPCB and MCPCB are 2.0 °C and 0.9 °C, respectively. Although the bottom temperature uniformity of the MEPCB is a little worse than that of the MCPCB, the average bottom temperature is still 1.8 °C larger than that of the MCPCB. It indicates that the heat can be better transferred to the bottom of the circuit board from the LED component, therefore enhancing the heat dissipation efficiency.

Thermal resistance is an important attribute for evaluating the LED device. The simulated thermal resistances from the LED chip to the bottom ($R_{\text{th,j-btm}}$) of the MEPCB and MCPCB are also evaluated by the following equation:

$$R_{\text{th j-btm}} = \left(T_{\text{j}} - T_{\text{btm,avg}}\right)/P_{\text{th}}. \tag{8}$$

Here, P_{th} is equal to the heat consumption of 1 W as mentioned in Section 2.2. The $R_{\text{th,j-btm}}$ of MCPCB is 27.2 K/W from the simulated result. The large thermal resistance means that this insulating layer seriously blocks the heat flow transferring from the LED component to the aluminum layer. Thus, the heat conduction advantage of the aluminum layer has been greatly weakened. As a contrast to the MCPCB, there is no low

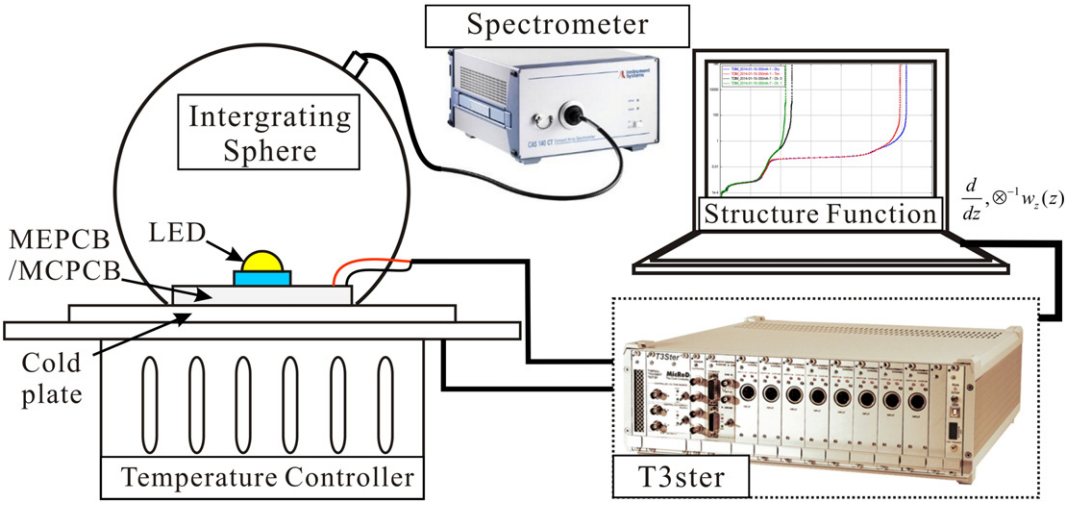

Fig. 2. Schematic diagram of measurement setup.

thermal conductivity material blocking in the heat dissipation path in the MEPCB. Therefore, the heat can be transferred from the LED component to the bottom side rapidly. The simulated $R_{th,j\text{-}btm}$ of MEPCB is only 10.0 K/W. The difference of the $R_{th,j\text{-}btm}$ between the MCPCB and MEPCB is 17.2 K/W, which can be mainly ascribed to the insulating layer.

3.2. Measured thermal performances

The *K* factor of the LED used in this work is −0.78 °C/mV at a measurement current of 5 mA according to the Eq. (4) as shown in Fig. 5. This means that the forward voltage would drop 1.28 mV when the junction temperature rise 1 °C. A cumulative structure function defined as the sum of *dC* with respect to the sum of *dR* is revealed in Fig. 6 at the input current of 350 mA and cold plate temperature of 25 °C. It is noticed that there are three separation points: A, B and C. These points mean that the heat flow is beginning to enter different layers whose capacitance and thermal resistance are rather different. The following results can be observed. 1) On the left of point A, the four cumulative structure function curves run analogously, which means that the heat flow paths of the two samples are the same. Once the curves pass point A, the heat flow will enter the upside surface of the circuit board because it is the first different layer between the thermal paths of the two samples. The abscissa value of point A represents the thermal resistance from the LED chip to the upside surface of the MCPCB or MEPCB, which is the so called LED component thermal resistance, and the value is 8.6 K/W; and 2) since the thermal grease decreases the contact thermal resistance between the LED device and the cold plate, the cumulative structure function curves separate at points B and C. The abscissa value from A to B represents the thermal resistance of MEPCB (2.1 K/W), which is mainly attributed to the copper slug. The abscissa value from A to C represents the thermal resistance of MCPCB (20.0 K/W), which includes the thermal resistances of insulating layer (16.9 K/W) and aluminum layer (3.1 K/W). It can be found that the major portion of the thermal resistance of MCPCB comes from the insulating layer. The conspicuous difference of the thermal resistance between the MEPCB and the MCPCB indicates that the insulating layer indeed blocks the heat flow greatly as inferred from the simulation results.

The thermal resistance from junction to ambient (cold-plate) without applying thermal grease is defined as the total thermal resistance ($R_{th,j\text{-}a}$). Fig. 7 reveals the $R_{th,j\text{-}a}$ versus supplied powers. It is noticed that the MEPCB LED component has much lower $R_{th,j\text{-}a}$ at different supplied power levels than that of the MCPCB. And the difference of the $R_{th,j\text{-}a}$ between the MEPCB and MCPCB increases with the input currents. For example, at about 0.5 W (150 mA), the $R_{th,j\text{-}a}$ of the MEPCB is 20.0 K/W, which is 16.0 K/W lower than that of the MCPCB. At about 3.5 W (900 mA), the $R_{th,j\text{-}a}$ of the MEPCB reaches the lowest of 11.8 K/W and it is 22.5 K/W lower than that of the MCPCB. The maximum reduction in the thermal resistance is 65.60%. This is mainly because that the $R_{th,j\text{-}a}$ is not constant with supplied powers. The $R_{th,j\text{-}a}$ of MEPCB keeps decreasing with the increasing power, while that of the MCPCB decreases at low powers and then increases at high powers. A reasonable explanation for the $R_{th,j\text{-}a}$ decreasing is that the active area of the chip changes with

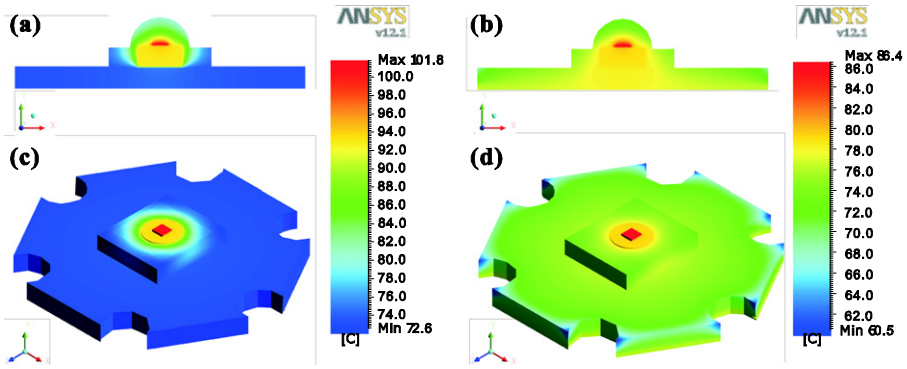

Fig. 3. Simulated thermal maps of MCPCB and MEPCB LED component showing the temperature distributions, (a) cross section view of the MCPCB, (b) cross section view of the MEPCB, (c) axonometric view of the MCPCB, and (d) axonometric view of the MEPCB.

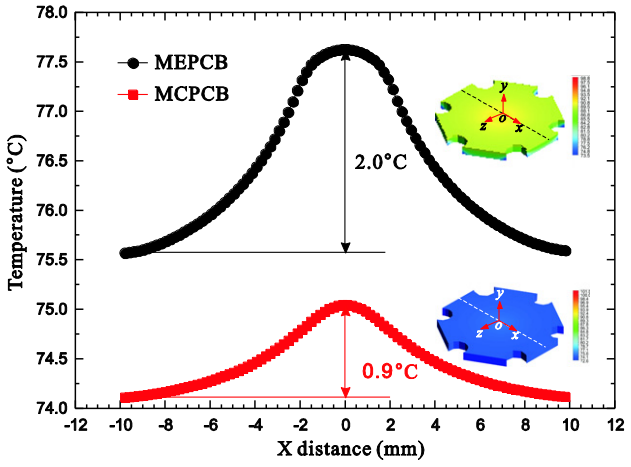

Fig. 4. The temperature distribution at the bottom surface of the MEPCB and the MCPCB.

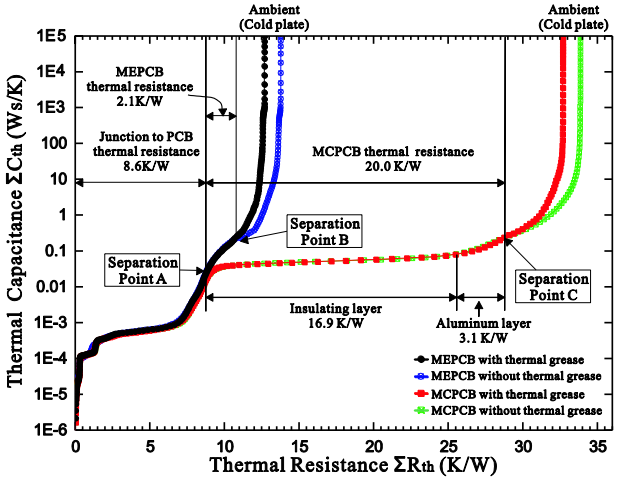

Fig. 6. Cumulative structure functions of MEPCB and MCPCB base LED component at input current of 350 mA.

the currents, which is known as current crowding effect [23–25]. At low supplied powers, the input current is low, and only part of the active layer of the LED chip actually carries the current. The small area of the heat source leads to the relatively high effective thermal resistance of the LED chip. With the supplied power increasing, larger active area is conducted and the heat is spread more uniformly through the chip. Consequently, the effective thermal resistance of the LED chip decreases. When the supplied power keeps increasing, the junction temperature will rise greatly for the LED on the MCPCB. For example, the junction temperature of the MCPCB at about 3.5 W (900 mA) rises to 144.0 °C as shown in Fig. 8, which has exceeded the recommended maximum temperature of the chip. The high junction temperature will lead to more serious nonradiative recombination in LED chips [26]. Thus, the current crowding effect, which increased the total thermal resistance, may occur again [27]. As for the MEPCB, the junction temperatures can be well controlled in an acceptable temperature range. For example, at about 3.5 W (900 mA), the junction temperature of the LED on the MEPCB is 63.0 °C, 56.25% lower than that of the MCPCB. The total thermal resistance ($R_{th,j\text{-}a}$) of the MEPCB at the supplied power above 3 W (750 mA) does not firm up. This indicates that the current crowding effect may not occur at high currents for the MEPCB.

Fig. 8 shows the junction temperature versus the supplied powers. It can be observed that the junction temperature of the MCPCB is more sensitive with the supplied powers than that of the MEPCB. Especially at high supplied powers, increasing power will change the junction temperature greatly for the MCPCB. There is a dividing power about 1.5 W (450 mA). When the power is below 1.5 W, the junction temperature rises linearly. Conversely, when the power is above 1.5 W, the junction temperature rises exponentially. It indicates that the MCPCB is only fit for low supplied powers. For the MEPCB, the junction temperatures rise linearly with the supplied powers, and always keep in lower values compared with the MCPCB. From about 0.5 W (150 mA) to 3.5 W (900 mA), the junction temperature changes from 32.3 °C to 63.0 °C, with an increase of only 30.7 °C. It means that, even if the supplied power changes a lot, the junction temperature of the LED on the MEPCB can be still kept in an acceptable range. This is meaningful for high power LEDs working at wide power ranges. Supplying high power to the LED chip is one of the most efficient ways to enhance the light output. However, high supplied powers will increase the junction temperature inevitably, and therefore decrease the luminous efficiency, shift the wavelength and generate the color deviations. It is expected that, by using the MEPCB, the brightness and chromaticity shifts will be limited.

3.3. Electrical, luminous and chromatic performances

Transient and steady measurements are two major methods for LED assessment. In transient measurement, it takes a very short time (sub-millisecond time-scale) to measure the parameters. This meets the demand of high production efficiency for LED manufactures. Since the power-on time is rather short, the heat generated in LED chips can be

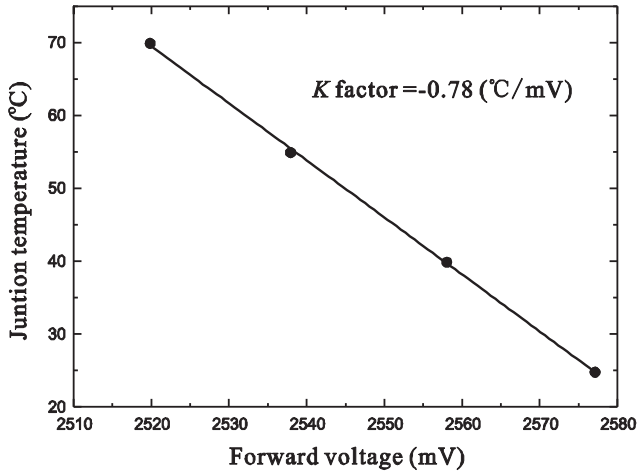

Fig. 5. Junction temperatures versus forward voltages at measurement current of 5 mA.

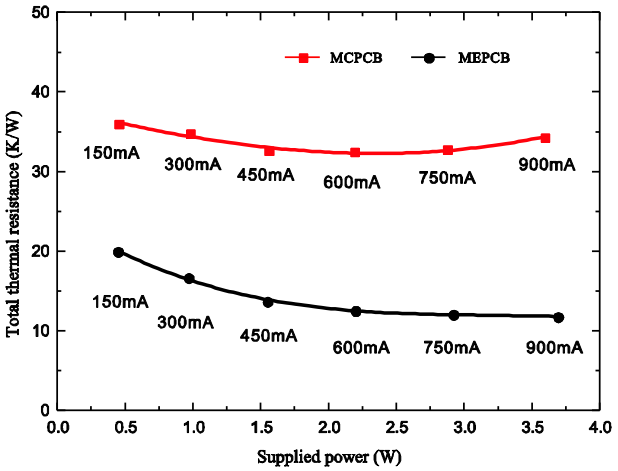

Fig. 7. Total thermal resistances versus supplied powers.

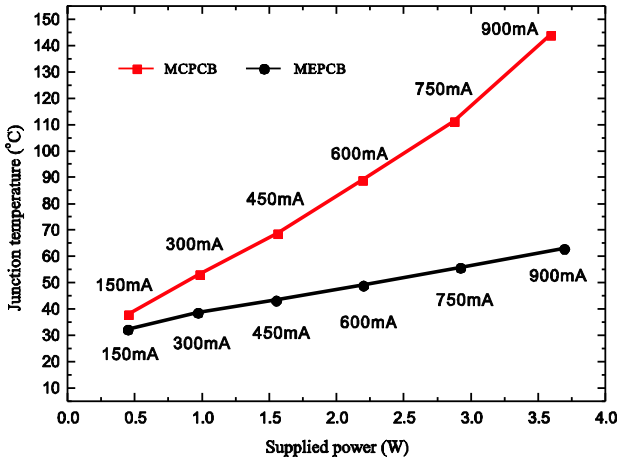

Fig. 8. Junction temperatures of the LED chips versus supplied powers.

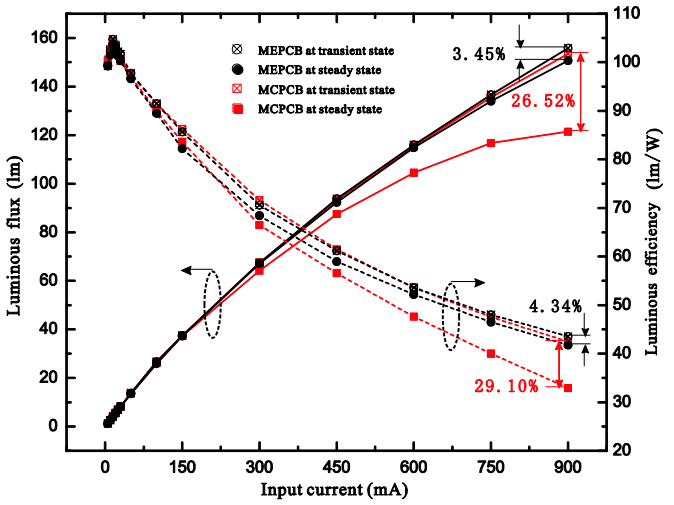

Fig. 10. Transient state and steady state luminous flux and efficiency versus input currents.

neglected. However, such a measurement method does not match with the real applications to some extent. Temperature rise of LED chip inevitably affect the light output performance under different conditions. For this reason, steady measurement is employed. LEDs are powered on to a thermal steady state, and then the parameters are measured. This method takes into full account for the influence of temperature change, but consumes a long time. That makes it not suitable for online test in mass production. Generally, by comparing the transient and steady measurement results, the luminous and chromatic stabilities can be obtained, which is an auxiliary evident of LED thermal behaviors. Fig. 9 shows the forward voltages of MEPCB and MCPCB versus input currents. It is noted that the forward voltages at steady state are lower than that at transient state. Obviously, the decreases of the forward voltages from transient states to steady states on MCPCBs are much larger than those on MEPCBs, which qualitatively implies that the LEDs on MEPCBs have the better thermal performance.

Luminous efficiency (η) is an important parameter to evaluate the optical performance, which can be calculated by Eq. (9).

$$\eta = \Phi_v / P_{el} \tag{9}$$

where Φ_v is the output luminous flux, and P_{el} is the total electrical power. The measured luminous efficiencies of the LEDs on the MEPCB and MCPCB at transient states and steady states are revealed in Fig. 10. With the increase of input current, the luminous efficiencies increase at first and then decrease. The maximum efficiency appears at the input current around 20 mA. At the highest current of 900 mA, the luminous efficiencies of the MCPCB decrease by 9.58 lm/W (29.10%) from transient state to steady state, while that of the MEPCB only decreases by 1.85 lm/W (4.34%). From Eq. (9), it can be inferred that there are two reasons for the decrease of the luminous efficiency from transient state to steady state: 1) the increase of the input power; and 2) the decrease of the luminous flux. Interestingly, on the premise of constant current cases, even though the decrease of the forward voltage of the MCPCB case is larger than that of the MEPCB case, the luminous efficiency decrease is still more serious. The only appropriate explanation is that the decrease of the luminous flux from transient state to steady state of the LED affects the total luminous efficiency as a dominant role. According to the luminous fluxes in Fig. 10, no matter using transient or steady measurement, the luminous fluxes of the MEPCB and MCPCB increase with the increasing input currents, but the increasing slopes decrease. At transient state, the luminous fluxes of the MEPCB and MCPCB are very similar at different currents. At steady state, the luminous fluxes are lower than that at transient state for both samples. And the luminous flux differences between the two components become distinct, especially at high currents. For the MCPCB, the transient state and steady state luminous flux curves started to separate clearly when the input current is above 300 mA. And at 900 mA, they are 153.6 lm and 121.4 lm, respectively. For the MEPCB, the increasing trend of the luminous flux at steady state is similar with that at transient state. At 900 mA, the luminous fluxes in the transient state and steady state are 155.9 lm and 150.7 lm, respectively. The MEPCB can enhance the luminous flux by 29.3 lm (24.14%) compared with the MCPCB, which means that the MEPCB can help LEDs to obtain high brightness in high power applications.

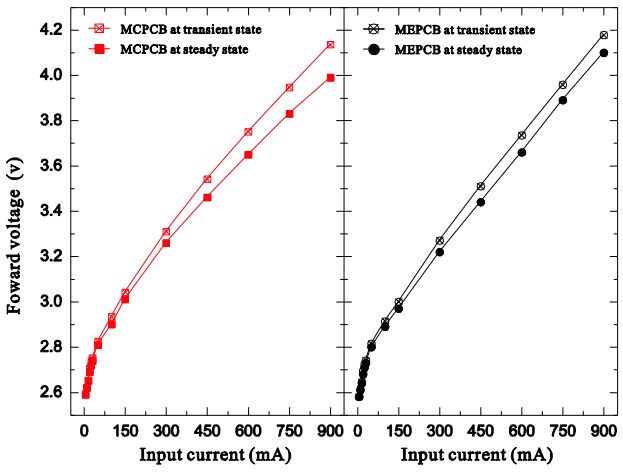

Fig. 9. The forward voltage variation with the input current for the MCPCB and MEPCB.

With the increasing requirement of high quality LED lightings, the chromatic performance becomes more and more important. Fig. 11 shows the chromaticity coordinates at the transient state and steady state chromaticity coordinates under different input currents. In order to simplify the discussions, the correlated color temperature (CCT) shift value versus current (from 150 mA to 900 mA) is defined as C-shift; and the CCT shift value between the transient state and steady state is defined as TS-shift. For the transient measurement, the CCTs of the MEPCB and MCPCB samples shift toward to high color temperatures almost linearly and parallelly with the increasing input currents. This is because that the blue light emission from the LED chip increases with the increasing current, leading to the chromatic coordinates shifting to the blue part in the chromaticity diagram, which is also known as blue shift. The C-shifts of the LEDs on the MEPCB and MCPCB are 77 K and 83 K, respectively. For the steady measurement, the C-shifts of the LEDs on the MEPCB and MCPCB are 93 K and 223 K with the input

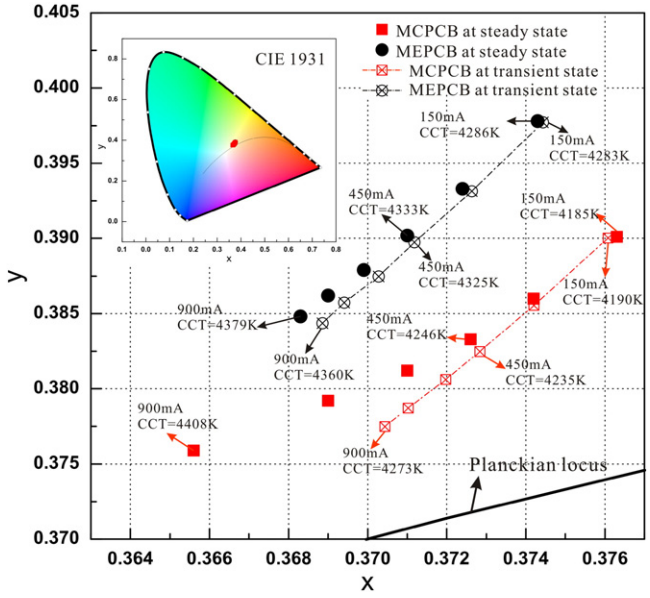

Fig. 11. Transient state and steady state chromaticity coordinates of the MCPCB and MEPCB at different input currents.

current from 150 mA to 900 mA, respectively. The relationships of the chromatic coordinates versus currents have become nonlinear. It can be also obtained that the C-shift of the MCPCB is more serious than that of the MEPCB. Compared with the transient state results, the TS-shifts increase with the increasing current for both LEDs on the MEPCB and MCPCB. The largest TS-shift of the LED on the MEPCB is 19 K at 900 mA, while it is 135 K for the LED on the MCPCB. A reasonable explanation for the above results is that the high temperature will decrease the blue emission and the phosphor excitation efficiency, but the latter loses more from our previous research [28], which leads to a more serious blue shift for the LEDs at high currents. For high current cases, the chromaticity of the LEDs on MCPCB will be very different with the nominal value measured at transient state. Obviously, the MEPCB can keep the C-shift and TS-shift within acceptable ranges. The reduction of chromatic shift within a wide range of input current is meaningful for LED light quality, especially in the coming intelligent lighting age.

4. Conclusions

In conclusion, a metal embedded printed circuit board has been developed in this work. Finite element analysis and transient thermal measurements were used to evaluate the thermal performances, including the thermal resistances, the junction temperatures and the temperature uniformities. Finally, the luminous and chromatic performances were also measured as further evident of the thermal behaviors.

The FEA results demonstrate that the heat flow can be effectively dissipated through the embedded copper slug to the bottom copper layer. The simulated thermal resistances well match with the transient thermal measured results. The total thermal resistance of the MEPCB decreases with the increasing current monotonically, which indicates that the current crowding effect may not occur at high currents. At the supplied power of about 3.5 W (900 mA), for the MEPCB, the total thermal resistance from LED junction to ambient is 11.8 K/W and the junction temperature is 63.0 °C, which are 65.60% and 56.25% lower than the conventional MCPCB. Benefiting from the excellent thermal performance of the MEPCB, up to 24.14% increase in steady state luminous flux is obtained compared with the MCPCB. It is also found that the decrease of the luminous flux from transient state to steady state is the dominant reason for the luminous efficiency reduction. Moreover, the MEPCB can also improve the chromatic stability of the LED by reducing the C-shift and the TS-shift, which is very important for high quality lightings.

Printed circuit boards play important roles in LED lightings. In order to enhance the thermal and optical performances of the high power LEDs, and take the cost into account, new types of printed circuit boards have to be developed. This paper gives a detailed evaluation on the novel MEPCB, and proves that the MEPCB is more suitable for LEDs working at wide current ranges.

Acknowledgments

This work is financially supported by the National Natural Science Foundation of China, No.51375177, No.U1401249 and No.51405161 and the Science and Technology Program of Guangdong Province, No. 2011A081301006.

References

[1] E.F. Schubert, J.K. Kim, Solid-state light sources getting smart, Science 308 (2005) 1274–1278.
[2] J. Cho, E.F. Schubert, J.K. Kim, Efficiency droop in light-emitting diodes: challenges and countermeasures, Laser Photonics Rev. (2012) 408–421.
[3] W.-H. Chi, T.-L. Chou, C.-N. Han, S.-Y. Yang, K.-N. Chiang, Analysis of thermal and luminous performance of MR-16 LED lighting module, IEEE Trans. Compon. Packag. Technol. 33 (2010) 713–721.
[4] N. Narendran, Y. Gu, Life of LED-based white light sources, J. Disp. Technol. 1 (2005) 167–171.
[5] T. Jeong, K.H. Kim, S.J. Lee, S.H. Lee, S.R. Jeon, S.H. Lim, J.H. Baek, J.K. Lee, Aluminum nitride ceramic substrates-bonded vertical light-emitting diodes, IEEE Photon. Technol. Lett. 21 (2009) 890–892.
[6] L. Yang, S. Jang, W. Hwang, M. Shin, Thermal analysis of high power GaN-based LEDs with ceramic package, Thermochim. Acta 455 (2007) 95–99.
[7] J.K. Park, H.D. Shin, Y.S. Park, S.Y. Park, K.P. Hong, B.M. Kim, A suggestion for high power LED package based on LTCC, Electronic Components and Technology Conference, Proceedings. 56th, IEEE 2006, pp. 441–444.
[8] J. Barcena, J. Maudes, M. Vellvehi, X. Jorda, I. Obieta, C. Guraya, L. Bilbao, C. Jimenez, C. Merveille, J. Coleto, Innovative packaging solution for power and thermal management of wide-bandgap semiconductor devices in space applications, Acta Astronaut. 62 (2008) 422–430.
[9] X. Jorda, X. Perpina, M. Vellvehi, J. Coleto, Power-substrate static thermal characterization based on a test chip, IEEE Trans. Device Mater. Reliab. 8 (2008) 671–679.
[10] I. Kim, S. Cho, D. Jung, C.R. Lee, D. Kim, B.J. Baek, Thermal analysis of high power LEDs on the MCPCB, J. Mech. Sci. Technol. 27 (2013) 1493–1499.
[11] Y.-W. Kim, S.-M. Park, M.-S. Kim, J.-P. Kim, J.-B. Kim, S.-B. Song, Y.-S. Lim, Optimization of flexible substrate for COF (chip on flexible) LED packaging, Electronic Components and Technology Conference, 59th, IEEE 2009, pp. 1953–1960.
[12] J.-Y. Wu, C.-M. Chen, R.-H. Horng, D.-S. Wuu, An efficient metal-core printed circuit board with a copper-filled through (blind) hole for light-emitting diodes, IEEE Electron Device Lett. (2013) 105–107.
[13] M.-H. Lee, T.J. Lee, H.J. Lee, Y.-J. Kim, Design and fabrication of metal PCB based on the patterned anodizing for improving thermal dissipation of LED lighting, Microsystems Packaging Assembly and Circuits Technology Conference, 5th International, IEEE 2010, pp. 1–4.
[14] N. Wang, A. Hsu, A. Lim, J. Tan, C. Lin, H. Ru, T. Jiang, D. Liao, High brightness LED assembly using DPC substrate and SuperMCPCB, Microsystems, Packaging, Assembly and Circuits Technology Conference, 4th International, IEEE 2009, pp. 199–202.
[15] K. Yung, H. Liem, H. Choy, W. Lun, Thermal performance of high brightness LED array package on PCB, Int. Commun. Heat Mass Transfer 37 (2010) 1266–1272.
[16] O. Calla, I.S. Rathore, Complex dielectric constant measurement of glass epoxy and zinc oxide at temperature ranging from −196 °C to 200 °C at microwave frequencies, J. Metall. Mater. Sci. 53 (2011) 161–173.
[17] J.-C. Wang, Thermal investigations on LED vapor chamber-based plates, Int. Commun. Heat Mass Transfer 38 (2011) 1206–1212.
[18] Z. Li, Y. Tang, X. Ding, C. Li, D. Yuan, Y. Lu, Reconstruction and thermal performance analysis of die-bonding filling states for high-power light-emitting diode devices, Appl. Therm. Eng. (2014) 236–245.
[19] V. Székely, T. Van Bien, Fine structure of heat flow path in semiconductor devices: a measurement and identification method, Solid State Electron. 31 (1988) 1363–1368.
[20] V. Székely, A new evaluation method of thermal transient measurement results, Microelectron. J. 28 (1997) 277–292.
[21] V. Szekely, Identification of RC networks by deconvolution: chances and limits, IEEE Trans. Circuits Syst. I, Fundam. Thoery Appl. 45 (1998) 244–258.
[22] JEDEC Standard, JESD51-14, Transient Dual Interface Test Method for the Measurement of the Thermal Resistance Junction to Case of Semiconductor Devices with Heat Flow Trough a Single Path, 2010.
[23] M. Bogdanov, K. Bulashevich, O. Khokhlev, I.Y. Evstratov, M. Ramm, S.Y. Karpov, Current crowding effect on light extraction efficiency of thin-film LEDs, Phys. Status Solidi C 7 (2010) 2124–2126.

[24] Y.Y. Kudryk, A. Tkachenko, A. Zinovchuk, Temperature-dependent efficiency droop in InGaN-based light-emitting diodes induced by current crowding, Semicond. Sci. Technol. 27 (2012) 1–5.
[25] X. Guo, E. Schubert, Current crowding in GaN/InGaN light emitting diodes on insulating substrates, J. Appl. Phys. 90 (2001) 4191–4195.
[26] N. Gardner, G. Müller, Y. Shen, G. Chen, S. Watanabe, W. Götz, M. Krames, Blue-emitting InGaN–GaN double-heterostructure light-emitting diodes reaching maximum quantum efficiency above 200 A/cm^2, Appl. Phys. Lett. 91 (2007) 243506.
[27] B.S. Siegal, Factors affecting semiconductor device thermal resistance measurements, Semiconductor Thermal and Temperature Measurement Symposium, Fourth Annual, IEEE 1988, pp. 12–18.
[28] Y. Tang, X. Ding, B. Yu, Z. Li, B. Liu, A high power LED device with chips directly mounted on heat pipes, Appl. Therm. Eng. (2014) 632–639.